

# Effect of Vanadium-Titanium Co-doping on the BPSCCO Superconductor

Duygu Yazıcı · Bekir Ozcelik · Serdar Altın ·  
M. Eyyüphan Yakıncı

Received: 8 September 2010 / Accepted: 9 September 2010 / Published online: 30 September 2010  
© Springer Science+Business Media, LLC 2010

**Abstract** We have produced the  $(\text{BiPb})_2\text{V}_x\text{Sr}_2\text{Ca}_3\text{Cu}_{4-y}\text{Ti}_y\text{O}_{12+\delta}$  compounds for  $x = 0.05$  and  $y = 0, 0.05, 0.10$  and  $0.20$  by glass-ceramic method. The effects of vanadium adding and Ti doping on the structure have been investigated by electrical resistance, scanning electron micrographs (SEM), XRD patterns and magnetic hysteresis loop measurements. It has been found that the high- $T_c$  superconducting phase, (2223), is formed in the samples annealed at  $845^\circ\text{C}$  for 185, with concentration  $x = y = 0.05$ . However, with increasing Ti doping the (2223) phase transforms into the (2212) phase. We have observed no superconducting properties for  $x = 0.05$  and  $y = 0.20$  compound. It has completely transformed to semiconductor.

In addition, the critical current densities ( $J_c$ ), calculated from the hysteresis loop measurements by using Bean's critical state model are obtained for the samples in the same doping range. Our data have indicated that  $J_c$  decreases with increasing temperature and Ti concentration.

**Keywords** Bi-based cuprates · XRD · SEM · Resistivity · BPSCCO

## 1 Introduction

As is well known there are three superconducting phases in the BPSCCO superconductor with an ideal structural formula

$\text{Bi}_2\text{Sr}_2\text{Ca}_{n-1}\text{Cu}_n\text{O}_{4+2n}$  where  $n$  represents the number of  $\text{CuO}_2$  layers. Each phase has a specific transition temperature to the superconductive state, and for  $n = 1$  (2201),  $T_c = 20$  K;  $n = 2$  (2212)  $T_c = 80$  K and  $n = 3$  (2223)  $T_c = 110$  K. In all high- $T_c$  ceramic superconductors, the  $\text{CuO}_2$  planes which contain magnetic  $\text{Cu}^{2+}$  ions, probably enhance the superconductivity, instead of degrading [1]. Weak coupling between  $\text{BiO}-\text{BiO}$  layers in the BPSCCO system enables the substitution of the different oxides for  $\text{Bi}^{3+}$  site. Some of the results have demonstrated that there is no significant increase in the  $T_c$ . But important changes occur in the carrier concentration due to the different cation doping levels. Therefore, the electrical property of the system varies.

It is rather difficult to achieve an isolated (2223) phase formation since the (2212) phase grows prior to the (2223) phase during synthesis [2, 3]. Therefore, synthesis of pure 2212 and 2223 phases in BPSCCO superconductor is important both from a technical and scientific point of view. Since this material is more elastic compared to other high- $T_c$  superconductors, it is preferred to make wires and cables working at liquid nitrogen temperatures [4, 5]. Much effort has been devoted to isolate (2223) phase by changing the nominal composition the some elements. When excess of Cu and/or Ca was introduced, it was observed that the fraction of (2223) phase increases [6]. Some elements have been partially substituted in order to improve formation and stability of the (2223) phase [7]. Among these, partial substitution of trivalent Bi with lead (Pb) has promoted the formation of the (2223) phase [8–10]. Lead atoms not only increase the hole concentration in the  $\text{CuO}_2$  planes but they also create empty places for oxygen atoms with +2 coordination number. The nominal composition of Pb was determined as 0.4 atomic percent [11, 12]. It was also reported that Pb atoms behave as efficient nucleation and growth sites for the for-

D. Yazıcı · B. Ozcelik (✉)  
Department of Physics, Faculty of Sciences and Letters,  
Çukurova University, 01330 Adana, Turkey  
e-mail: ozcelik@cu.edu.tr

S. Altın · M.E. Yakıncı  
Department of Physics, Faculty of Sciences and Letters, İnnönü  
University, 44069 Malatya, Turkey

mation of 2223 phase and enhance the diffusion of the calcium and copper atoms. There are a number of constraints in the synthesis of single (2223) phase. First of all, there are many cations in the BSCCO system. Since the mobility and reaction rate of these cations are different, homogeneous distribution of them is not easily achieved. As a result, reaction of two or more elements produces impurities, which decrease the (2223) fraction. Secondly, the phase-formation temperature of (2223) is very narrow and strongly depends on the initial composition [8, 13–15]. In addition, (2223) phase has a tendency to decompose to low- $T_c$  (2212) and (2201) phases at certain temperatures. Therefore, this makes it more difficult to understand the complicated mechanism involved in the (2223) formation process [16]. Finally, since the crystal structure of (2212) and (2223) is very similar, it often results in intergrowth of these phases in the material.

It has recently been observed that niobium, vanadium, and titanium addition increases the (2223) phase considerably and one succeeded to isolate this phase up to 96% and 97% [17, 18]. Here we should state that the preparation technique of a system is also very important. To this end preparing the BSCCO system by the glass-ceramic technique yields a good density and minimum porosity, compared to the conventional solid-state technique [19–22].

As stated in the previous paragraph it has now been well established that the superconducting properties of the copper oxide superconductors are related to the hole concentration. Nevertheless, there are few reports on the effects of substitutions to Cu site in the BSCCO (2223) system. In this study, we desire to investigate the effect of other high valancy cations which will make the same effect as Nb. For this reason, we have added vanadium to Bi-site and substituted titanium to Cu-sites independently and observed the (2223) phase variation.

## 2 Experimental Process

The appropriate amounts of  $\text{Bi}_2\text{O}_3$ ,  $\text{PbO}$ ,  $\text{TiO}_2$ ,  $\text{V}_2\text{O}_5$ ,  $\text{SrCO}_3$ ,  $\text{CaCO}_3$ , and  $\text{CuO}$  fine powders in the stoichiometric ratios of  $\text{Bi}_{1.6}\text{Pb}_{0.4}\text{V}_x\text{Sr}_2\text{Ca}_3\text{Cu}_{4-y}\text{Ti}_y\text{O}_{12+\delta}$  ( $x = 0.05$  and  $y = 0.0, 0.05, 0.1$ , and  $0.2$ ) were well mixed by milling and the resulting powders were placed in a platinum crucible and heated at  $1200^\circ\text{C}$  until the samples were completely melted. The melts were poured onto a pre-cooled copper plate and pressed quickly by another copper plate to obtain an approximately 1.5 to 2 mm thick plate like amorphous (glass) material. The mixture was re-grinded for about two hours and the resulting powders were then pressed into pellets of 13 mm diameter by applying a 5 tons pressure. Finally, the precursor materials produced were annealed at  $845^\circ\text{C}$  for 185 h in air to achieve crystallized material and superconductivity.

The samples with  $x = 0.05$  and  $y = 0.0, 0.05, 0.10$  and  $0.20$  will hereafter be named H, J, K, and L, respectively.

Resistivity measurements were carried out on our samples using a standard four-probe method with silver paint contact. X-ray powder diffraction analyses were performed by using a Rigaku RadB powder diffractometer system with  $\text{CuK}\alpha$  radiation and a constant scan rate between  $2\theta = 3$ – $60^\circ$  at room temperature, to examine the phases present in the samples. SEM photographs for the study of the microstructure were taken by using a LEO Evo-40 VPX scanning electron microscope (SEM) and a Röntec energy dispersive X-ray spectroscopy (EDX). The magnetic measurements were performed with a 7304 model LakeShore VSM.

## 3 Results and Discussions

The resistance ( $R$ ) versus temperature ( $T$ ) curves for all the samples, from 200 K down to 20 K are given in Figs. 1 and 2. For sample H, which has no Ti concentration, two onset transition temperatures occur with  $T_{c,\text{onset}1} = 118$  K and

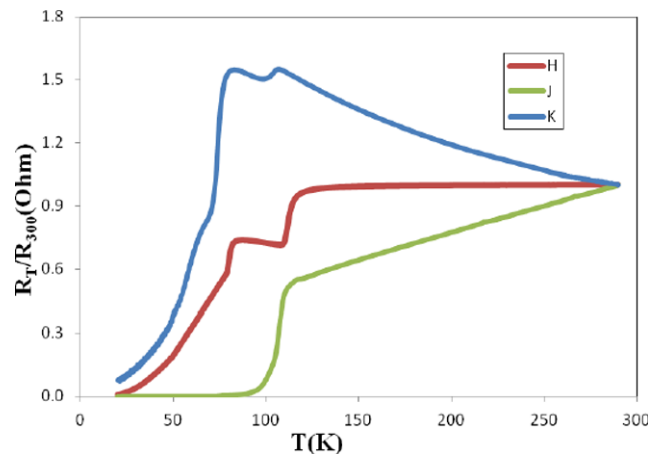


**Fig. 1** Temperature dependence of resistivity for samples H, J and K

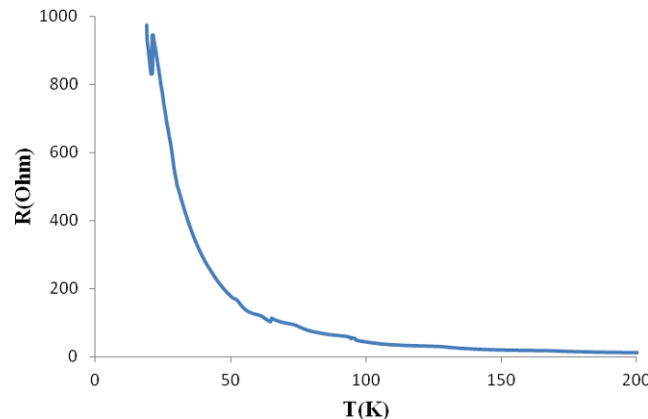


**Fig. 2** Temperature dependence of resistivity for sample L

$T_{c,\text{onset}2} = 89$  K and then  $R$  goes to zero at  $T_{c,\text{offset}} = 30$  K. For samples J, the  $T_{c,\text{onset}}$  (below which the sample is in a superconducting state) of superconductivity are about 109 K and R almost goes to zero at  $T_{c,\text{offset}} = 96$  K. Hence, there is the superconducting transition range  $\Delta T$  of about 13 K, which means the high- $T_c$  phase (2223) is the dominant phase in the samples. We should emphasize here that sample J seems to have the best value of the concentration for obtaining the (2223) phase. Sample K exhibits a semiconducting trend down to 115 K, and then a two-step superconducting transition is observed with a long tail. The sample L shows completely semiconducting behavior, which indicates insufficient superconducting phase formation. As a result, the H and K samples further increase in Ti concentration and this causes a broadening transition and a dramatic decrease of the  $T_{c,\text{offset}}$  values. This obviously indicates a weak grain coupling in the samples, and with increasing amount of Ti, this necessarily favors the formation of the (2212) phase with respect to the common (2223) phase.

The deduced  $T_{c,\text{onset}}$  and  $T_{c,\text{offset}}$  values from  $R-T$  measurements are tabulated in Table 1 for the samples H, J and K.

**Table 1** The  $T_c$  values deduced from the  $R-T$  data

Samples	$T_c$ (K)
H	$T_{c,\text{onset}} = 118$ and 89 K $T_{c,\text{offset}} = 48.1$ K
J	$T_{c,\text{onset}} = 109$ K $T_{c,\text{offset}} = 96$ K
K	$T_{c,\text{onset}} = 107$ and 80.3 K $T_{c,\text{offset}} = 44.6$ K

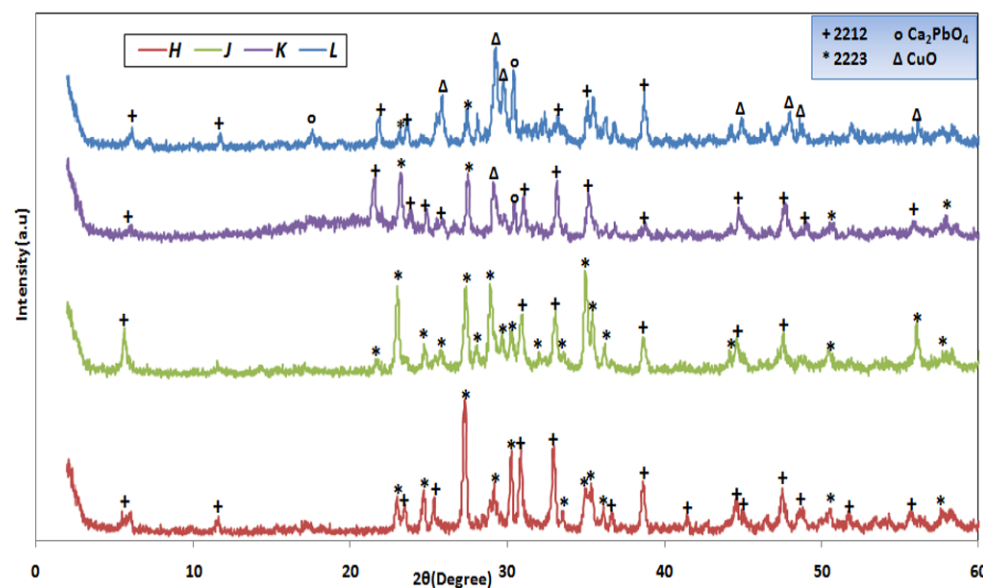
The XRD diffraction patterns of H, J, K and L samples are shown in Fig. 3. It is obvious that low- $T_c$  phase (2212) is dominant for the H and K samples, and the (2223) phase is the dominant one for sample J. As can be seen, non-superconducting CuO and Ca<sub>2</sub>PbO<sub>4</sub> phases occurred in all samples but these phases are only dominant for sample L. As a result, with increasing Ti concentration in the system, the superconducting phase is disturbed by the insulating phases. The phase coordination is destroyed and the multiphase, complex and deformed structures are obtained. The crystal symmetry of all the samples is found to be tetragonal. The calculated unit cell parameters of the samples are presented in Table 2.

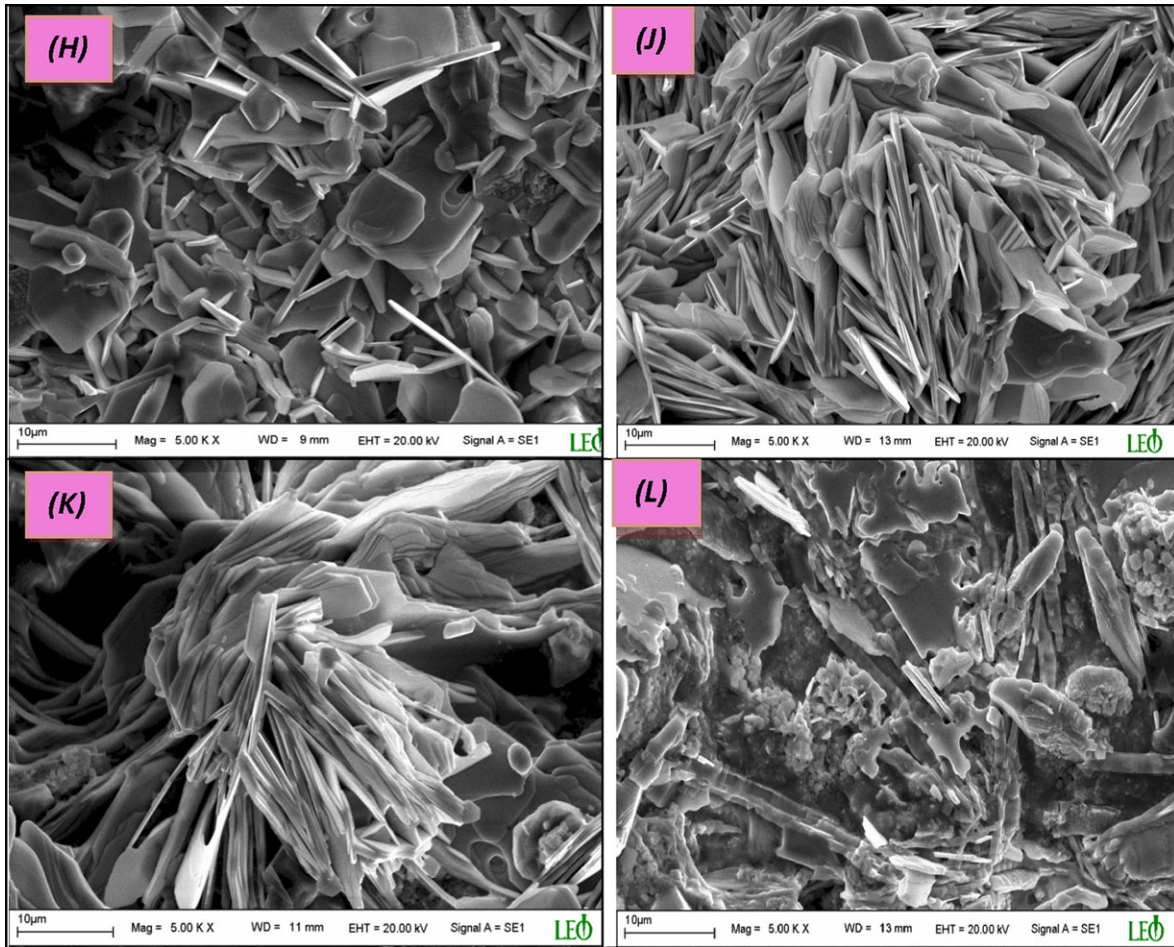
The SEM micrographs of the samples are illustrated in Fig. 4. Samples H and J contain both randomly oriented needle shapes and grain structure together with a small amount of porosity. Sample J has more uniform surface with a dense alignment of grains and needle-like crystals. It is seen that the surface composition of the sample J is closer to that of the Bi-(2223) phase. This is also confirmed by the  $R-T$  and XRD measurements given above. The density of porosities and non-superconducting structure are observed for sample K. This observation confirms our previous arguments that the K has almost the low- $T_c$  phase. In addition, the very

**Table 2** The calculated unit cell parameters of the samples

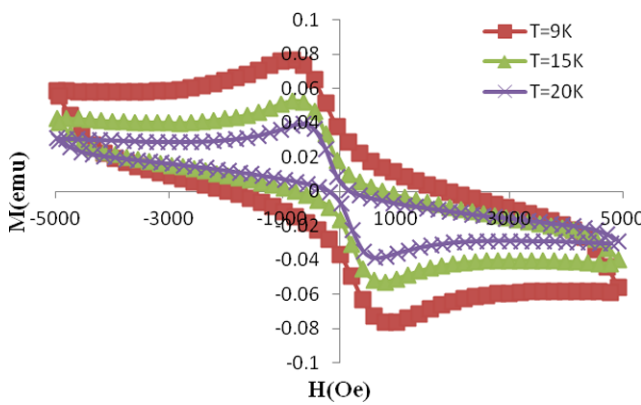
Samples	$a = b$ (Å)	$c$ (Å)
H	5.409	30.683
J	5.413	36.992
K	5.403	30.667
L	5.400	30.616

**Fig. 3** XRD result of H, J, K and L samples



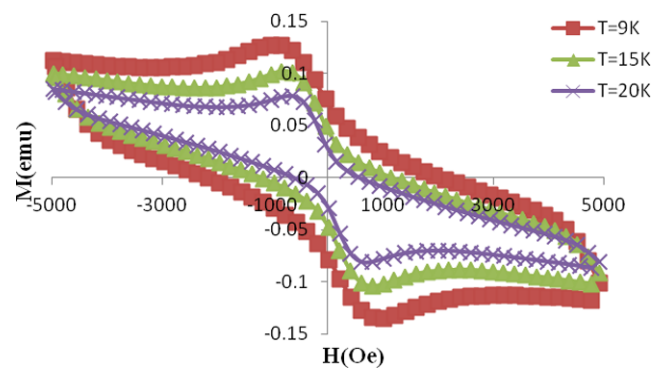


**Fig. 4** SEM photographs of the samples



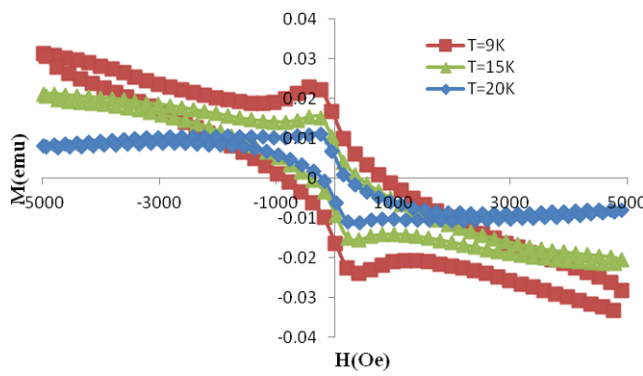
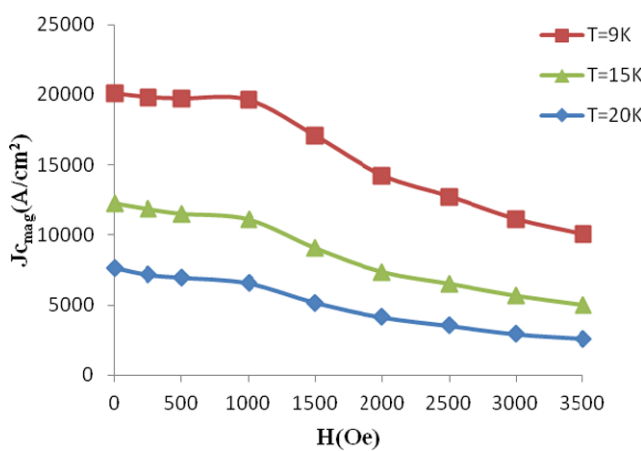
**Fig. 5**  $M$ – $H$  hysteresis of sample H

complex surface structure in which the general superconducting structure breaks down is observed for the sample L. It is argued that the crystallization temperature together with the melting point drops down with increasing Ti content. Therefore some kind of melted surface is observed in sample L.



**Fig. 6**  $M$ – $H$  hysteresis of sample J

The  $M$ – $H$  hysteresis loops for the samples, except L, are presented in Figs. 5–7 respectively. All those  $M$ – $H$  hysteresis loops were obtained after cooling the sample in zero magnetic field (ZFC) and measured between the fields of  $\pm 5$  kOe at the temperatures of 9, 15 and 20 K. Figure 6 demonstrates that the superconducting properties of

**Fig. 7**  $M$ - $H$  hysteresis of sample K**Fig. 8**  $J_{\text{cmag}}$  results of sample H

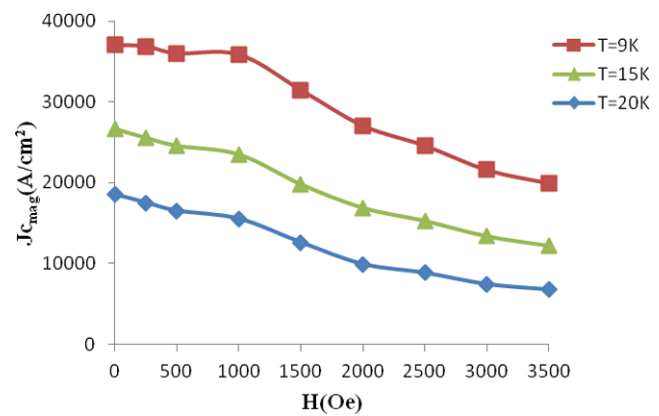
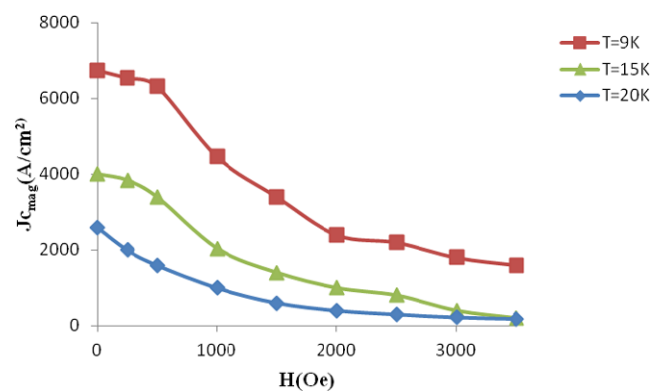
the sample J are much better than that of the others, since its hysteresis loop observed is much larger than the others.

The  $J_{\text{cmag}}$  values of the samples were determined using the Bean's model [23]:

$$J_{\text{cmag}} = 20 \frac{\Delta M}{a(1 - \frac{a}{3b})}$$

where  $J_{\text{cmag}}$  is the magnetization current density in ampères per square centimeter of a sample.  $\Delta M = M_+ - M_-$  is measured in electromagnetic units per cubic centimeter,  $a$  and  $b$  ( $a < b$ ) are the dimensions in centimeters of the cross-section of the sample parallel to the applied field.

The calculated critical current densities of the samples as a function of the applied field, at three different fixed temperatures, are shown in Figs. 8–10. As can be seen from Fig. 9 and Table 3, the maximum value of  $J_c$  ( $3.7 \times 10^4 \text{ A/cm}^2$ ) is obtained at 9 K for an optimally treated sample and then decreases with increasing temperature. H, J and K samples prepared show that the field dependence of  $J_{\text{cmag}}$  is strong even at 9 K (Figs. 8, 9 and 10). This kind of behavior can be explained in terms of weak grain connectivity and/or an increased volume fraction of impurity grains, such as formation of both BiPb-2212 and BiPb-2223 phases.

**Fig. 9**  $J_{\text{cmag}}$  results of sample J**Fig. 10**  $J_{\text{cmag}}$  results of sample K**Table 3**  $J_{\text{cmag}}$  result of samples H, J and K

Sample	$J_{\text{cmag}}$ at 9 K A/cm <sup>2</sup>	$J_{\text{cmag}}$ at 15 K A/cm <sup>2</sup>	$J_{\text{cmag}}$ at 20 K A/cm <sup>2</sup>
H	$2.0 \times 10^4$	$1.2 \times 10^4$	$0.76 \times 10^4$
J	$3.7 \times 10^4$	$2.6 \times 10^4$	$1.8 \times 10^4$
K	$0.67 \times 10^4$	$0.40 \times 10^4$	$0.26 \times 10^4$

In general, higher values of  $J_c$  have been calculated while a weak magnetic field dependence was still obtained at  $T > 9 \text{ K}$ . This is expected because the magnetization curve of the sample forms a loop that indicates the presence of pinning centers on the surface of the materials. It is also well known that in the high- $T_c$  superconducting material, non-superconducting impurity phases are highly effective in the flux-pinning mechanism. Thus, a higher critical current density with a small amount of non-superconducting phases is possible.

#### 4 Conclusion

In this study, the effect of vanadium adding and titanium substituting has been investigated. In addition we have not previously applied calcinations and milling process on the samples, just before the melting. The above results show that the substitutions vanadium and titanium enhances the superconducting properties of the pure (2223) phase for  $x = 0.05$  and  $y = 0.05$ . With increasing Ti doping the (2223) phase transforms into the (2212) phase and for the  $x = 0.05$  and  $y = 0.20$  compound no superconducting properties have been observed. It has completely transformed to a semiconductor.

**Acknowledgement** This work is supported by Reach Fund of Cukurova University, Adana, Turkey, under grant contracts no: FEF2009D11.

#### References

- Anderson, P.W.: Science **235**, 1196 (1987)
- Shi, D., Tang, M., Boley, M.S., Hash, M., Vandervoort, K., Claus, H., Lwin, Y.N.: Phys. Rev. B, Condens. Matter **40**(4), 2247 (1989)
- Sumiyama, A., Yoshimoto, T., Endo, H., Tsuchiya, J., Kijima, N., Mizuno, M., Oguri, Y.: Jpn. J. Appl. Phys. **27**(4), L542 (1988)
- Hellstrom, E.E.: In: Shi, D.L. (ed.) High Temperature Superconducting Materials Science and Engineering, p. 383. Pergamon, Elmsford (1994)
- Zeng, R., Beales, T.P., Liu, H.K., Dou, S.X.: Supercond. Sci. Technol. **11**(3), 299 (1998)
- Maeda, H., Tanaka, Y., Fukutomi, M., Asano, T.: Jpn. J. Appl. Phys. **27**(2), L209 (1988)
- Kanai, T., Kamo, T., Matsuda, S.: Jpn. J. Appl. Phys. **28**(4), L551 (1989)
- Chen, Y.L., Stevens, R.: J. Am. Ceram. Soc. **75**, 1150 (1992)
- Sunshine, S.A., Siegrist, T., Schneemeyer, L.F., Murphy, D.W., Cava, R.J., Batlogg, B., van Dover, R.M., Fleming, R.M., Glarum, S.H., Nakahara, S., Farrow, R., Krajewski, J.J., Zahurak, S.M., Waszczak, J.V., Marshall, J.H., Marsh, P., Rupp, Jr., L.W., Peck, W.F.: Phys. Rev. B, Condens. Matter **38**(1), 893 (1988)
- Ramesh, R., Green, S., Jiang, C., Mei, Y., Rudee, M., Luo, H., Thomas, G.: Phys. Rev. B, Condens. Matter **38**(10), 7070 (1988)
- Kijima, N., Endo, N., Tsuchiya, J., Sumiyama, A., Mizino, M., Oguri, Y.: Jpn. J. Appl. Phys. **27**, L821 (1988)
- Shi, D., Boley, M.S., Chen, J.G., Xu, M., Vandervoort, K., Liao, Y.X., Zangvil, A., Akujize, J., Segre, C.: Appl. Phys. Lett. **55**, 699 (1989)
- Endo, U., Koyama, S., Kawai, T.: Jpn. J. Appl. Phys. **27**(8), L1476 (1988)
- Tanaka, Y., Fukutomi, M., et al.: Jpn. J. Appl. Phys. **27**(4), L548 (1988)
- Tallon, J.L., Buckley, R.G., Gilberd, P.W., Preland, M.R.: Physica C **158**, 247 (1989)
- Suzuki, Y., Inoue, T., Huyashi, S., Komatsu, H.: Jpn. J. Appl. Phys. **28**(8), L1382 (1989)
- Sözeri, H., Ghazanfari, N., Özkan, H., Kılıç, A.: Supercod. Sci. Technol. **20**, 1 (2007)
- Yazıcı, D.: Ph.D. Thesis (2010)
- Ekicibil, A., Coşkun, A., Özçelik, B., Kiymaç, K.: Mod. Phys. Lett. B **18**(23), 1–12 (2004)
- Özkurt, B., Ekicibil, A., Aksan, M.A., Özçelik, B., Yakıncı, M.E., Kiymaç, K.: J. Low Temp. Phys. **147**, 31 (2007)
- Özkurt, B., Ekicibil, A., Aksan, M.A., Özçelik, B., Yakıncı, M.E., Kiymaç, K.: J. Low Temp. Phys. **149**, 105 (2007)
- Aksan, M.A., Yakıncı, M.E., Balcı, Y.: J. Supercomput. **15**(6), 553 (2002)
- Bean, C.P.: Phys. Rev. Lett. **8**, 250 (1962)